The Journal of Experimental Biology 207, 3569-3580
Published by The Company of Biologists 2004
doi:10.1242/jeb.01202

Models of hydrodynamic flow in the bowhead whale filter feeding apparatus

Alexander J. Werth

Department of Biology, Hampden-Sydney College, Hampden-Sydney, VA 23943, USA

e-mail: awerth@hsc.edu

Accepted 14 July 2004

Summary

Anatomical and behavioral analyses suggest that the filtration mechanism of bowhead and right whales (Balaenidae) is driven by hydrodynamic as well as ram hydraulic pressures. Complementary models were devised to investigate biomechanical aspects of water flow in the buccal cavity of the bowhead whale *Balaena mysticetus* during continuous filter feeding. A mathematical model was created to test and quantify water flow predictions with steady state hydromechanical equations; a physical model of the bowhead mouth (approximately 1/15 scale) was constructed to visualize flow processes. Both models rely on morphometric data obtained from whales harvested by Inupiat Eskimos for subsistence purposes along with information on foraging ecology (locomotor velocity, gape, etc.). Results indicate that unique features of balaenid oral construction and function (e.g. subrostral gap, orolabial sulcus, curvature of baleen, extensive mandibular rotation and lingual mobility) not only permit steady, unidirectional flow of water through the mouth, but also establish Bernoulli and Venturi effects during feeding. These hydrodynamic conditions allow balaenids to improve filtering efficiency and avoid creation of an anterior compressive wave (by increasing flow velocity and thereby reducing pressure) so that they may capture elusive prey even at slow swimming speeds.

Key words: bowhead whale, *Balaena mysticetus*, water flow, buccal cavity, baleen, tongue, feeding mechanism, morphology, filtration, flow, hydrodynamics.

Introduction

Balaenid (bowhead and right) whales are continuous filter feeders, in which a steady current of prey-laden water enters the mouth anteriorly between paired racks of baleen, passes through the baleen plates that comprise the sieving apparatus, and exits the oral cavity lateral to the pharyngeal orifice at the trailing edge of the lips (Figs 1–4). Unlike other mysticetes, which are intermittent filter feeders that ingest and process discrete mouthfuls of water by locomotor lunging (in the case of rorquals, Balaenopteridae, such as fin and humpback whales) or intraoral suction generation (in the gray whale, Eschrichtiidae) balaenids skim dense slicks of copepods and other tiny zooplankton while slowly cruising through all levels of the water column, including the surface and bottom (Pivorunas, 1979; Werth, 2000). The enormous head, constituting one third of a rotund, fully grown adult's 15–20 m length, functions as an immense plankton tow net (as in other continuous filter feeders, e.g. manta rays and whale and basking sharks), although this 'net' is not pulled along but rather propelled by the whale's forward locomotion at feeding speeds of 3–9 km h^{-1}.

Just as the elastic gular pleats, loose mandibular joint and flaccid, deformable tongue of rorquals reflect their lunge feeding, balaenid oral morphology is well designed for continuous sieving of microscopic prey (Fig. 1). The subrostral gap (a cleft between baleen racks below the tip of the rostrum) and orolabial sulcus (a gutter-like depression medial to the lip), which are specific features of the balaenid oral cavity designed exclusively to promote continuous, unidirectional water flow, are singular among mysticetes, as are the exceptionally long (up to 4 m), springy, finely fringed baleen (35–70 fringes m^{-2}), fused cervical vertebrae, firm tongue and high semicircular lips, extending well above the mandibles to enfold the narrow, arched rostrum (Werth, 2001).

Based on their description of the gross and microscopic structure of bowhead whale *Balaena mysticetus* baleen, Lambertsen et al. (1989) suggested that the filtration mechanism of balaenid feeding is powered not merely by hydraulic but also by hydrodynamic pressures. Their photogrammetric study documented the ability of the lower jaw and lip to rotate outward during feeding, creating a distinct channel for water flow along the outside of the baleen, which, when coupled with the convex lateral profile of the baleen rack, could cause lower pressures to develop outside the baleen, thereby drawing water from the buccal cavity through the sieve to improve filtering efficiency while also eliminating a compressive bow wave in front of the mouth.

Numerous restrictions (legal, logistical, fiscal, etc.) prevent direct experimentation on bowhead filter feeding; even close observation of feeding is now precluded by limited physical approach to live whales. However, observing bowhead feeding

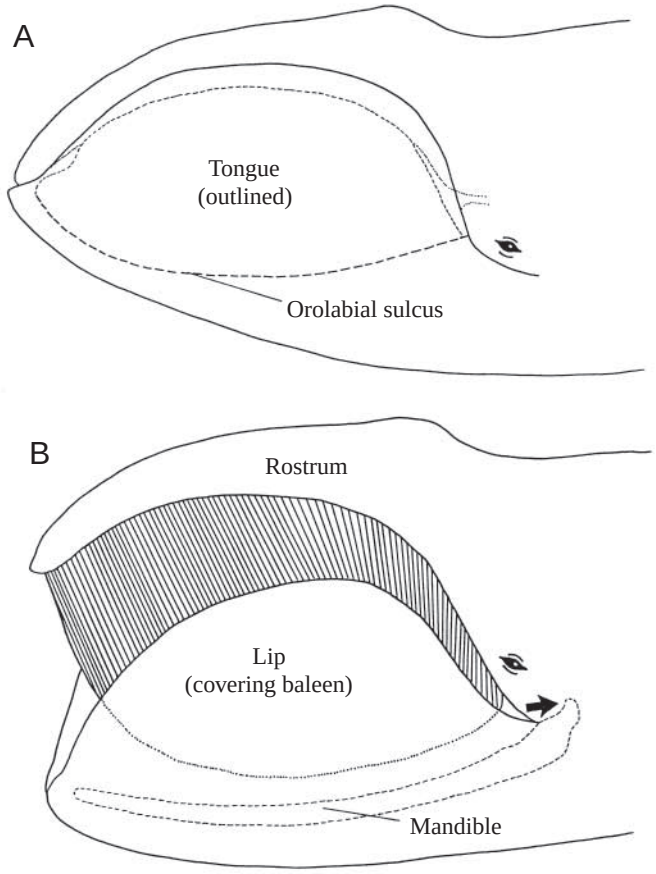

Fig. 1. Morphology of balaenid head. Schematic lateral views showing the narrow, arched rostrum and huge, scoop-shaped, lower jaw with mouth closed (A) and open, in feeding position, with abducted lips (B). (A) When the mouth closes the baleen folds back, the lip overlaps the upper jaw, and the central furrow of tongue (light broken lines) contacts the palate. Heavy broken lines indicate the orolabial sulcus between tongue and lip; the dotted line denotes oropharynx and esophageal orifice. (B) In the less streamlined open-gape feeding profile, note the large lower lip above the mandible (broken line) and the overlapping extent of the freely suspended baleen rack (dotted line), with the shortest plates at rear. The arrow indicates where filtered water exits posterior to the lip after passing along the gutter-like orolabial sulcus.

from a kayak, Otto Fabricius reported in 1780 that planktonic prey seemed to move into the whale's mouth as if attracted to it. In his monograph on Greenland fauna (Fabricius, 1780), he wrote: "*In this respect must Nature be admired, that these crustaceans find pleasure in its whalebones, seek there from all directions and go in more or less by themselves*".

Accordingly, a pair of distinct yet complementary morphological models was created to investigate biomechanical aspects of water flow in the bowhead oral cavity during continuous ram filter feeding. A conceptual mathematical model was designed to test and quantify predictions of hydrodynamic effects of flow with steady state hydromechanical conditions. In addition, a 1/15 scale physical model of the bowhead oral cavity (Fig. 2) was constructed to test and better visualize these processes in a flow chamber. Both models rely on morphometric and anatomical data obtained from adult and fetal bowhead whales harvested for subsistence purposes by Inupiat Eskimos near Point Barrow, Alaska, as well as from information concerning bowhead foraging ecology.

Materials and methods

Morphometrics

Data collection

Data used to construct the fluid mathematical and scale physical models came from examination of eight female bowhead whales *Balaena mysticetus* L. taken by native Inupiat Eskimos of Barrow, Alaska during the spring subsistence hunts of 1992–1995. These eight specimens included both adult and sexually immature whales (based on total body length, L_b, and gonadal interpretations) ranging from 9.21–15.85 m L_b. Whales were examined while hauled out on the ice, in fresh state and normal (prone) position, prior to and during

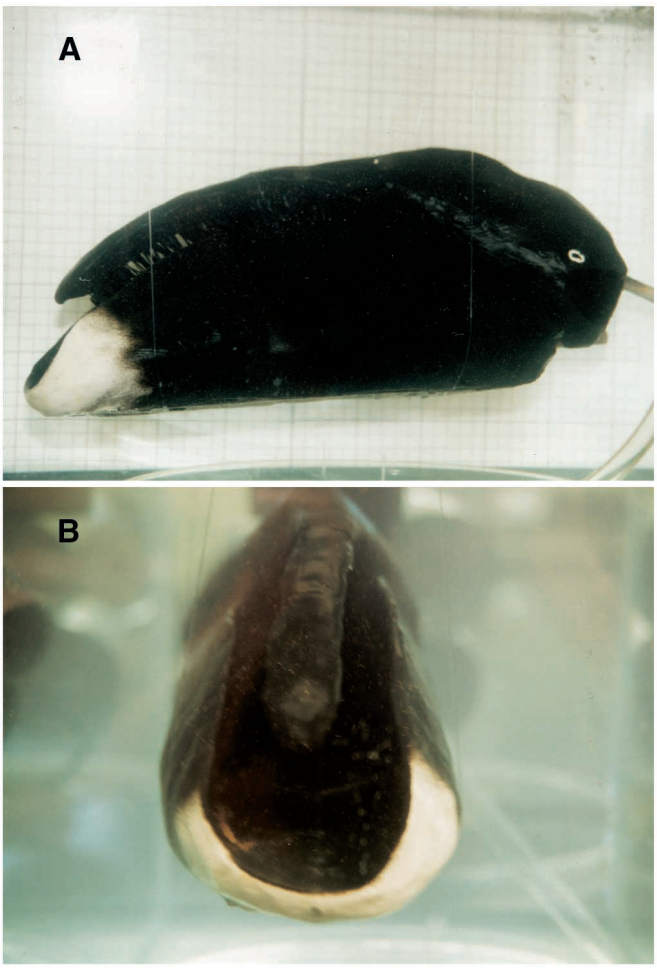

Fig. 2. Anterior (A) and lateral (B) views of 1/15 scale model of bowhead mouth photographed in the flow chamber before videotaping. Compare to other figures for descriptions of morphology.

butchering. Necropsy procedures were coordinated by the Department of Wildlife Management of the North Slope Borough (DWM/NSB), AK, USA and the Alaska Eskimo Whaling Commission (AEWC), using a standardized protocol described by Albert (1981) and Becker et al. (1991). Before the Inupiat hunters removed baleen and harvested other oral tissues, measurements were taken using a tape measure of the baleen, lips and tongue *in situ*. Structures were photographed, videotaped and sketched with scale bars for later study and measurement.

Two principal dimensions (dorsoventral in the mid-sagittal plane, denoted here as vertical; and in the frontal plane, or horizontal) were obtained for the anterior opening of the mouth as well as the mouth's paired posterior openings where filtered seawater exits the oral cavity posterior to the lips (Fig. 3). For the anterior opening, the dorsoventral or vertical (AV) measurement was defined as the distance between the tip of the upper jaw (at the subrostral gap between anteriormost baleen plates) straight down to the floor of the mouth, just at the anterior tongue tip; the anterior frontal or horizontal (AH) measurement was between the lowest points of the anteriormost baleen plates, where they touched the medial sides of the lips as they hung down. Measurements of the posterior mouth openings were defined as follows: posterior horizontal (PH), from the rear of the lip across the orolabial sulcus (the gutter-like depression posterior to the lip) to the head at the level of the eye; posterior vertical (PV), from the bottom of the orolabial sulcus up to the upper jaw, at the approximate midline of the PH dimension. As all measurements were recorded, gape was open to its normal feeding position (approximately 20% of body length), as ascertained from photographs of feeding whales and as judged by (1) AV length relative to L_b and (2) relative disclosure of baleen.

Given the clear landmarks described above, accuracy of measurement (both at the harvest site as well as during later confirmation by analysis of scaled photographs) was assured. Nonetheless, of the eight whales examined for this study, reliable measurements of oral structures and dimensions could be obtained from only five specimens. The other three whales were either turned slightly on their sides during harvesting, so that the lips rotated medially or laterally, or so that the gape was not open to its normal position during feeding, or else key structures were damaged during haulout or harvesting, in all three cases rendering some measurements suspect. Scaling the measurements of all whales to a standard 15 m L_b (using a 14.99 m long whale, 93B6) confirmed that these dimensions naturally scale linearly (almost perfectly isometrically), negating any possible allometric effects that could affect the dimensions and hence the construction of the mathematical or physical models.

Use in constructing models

The paired perpendicular dimensions (horizontal and vertical) of the anterior and posterior mouth openings were taken, loosely, as diameters for these roughly circular apertures. Accordingly, the average of both measurements [(AV+AH)/2] was taken as a mean diameter, from which the approximate radius of each orifice could be calculated.

Additionally, two fetal bowhead specimens were used in this study (88KK1F, L_b=1.5 m, collected from a 14.9 m female on 9/24/88 at Kaktovik, AK; 90B4F, L_b=3.9 m, from a 14.9 m female on 5/19/90 at Barrow, AK), representing mid-term and near-term gestational stages. Both fetuses were whole-body formalin-perfused through umbilical vessels and delivered from DWM/NSB to the Department of Veterinary Anatomy and Fine Structure, Louisiana State University School of Medicine, where they were examined, measured and dissected. Unfortunately, allometric growth of numerous features (e.g.

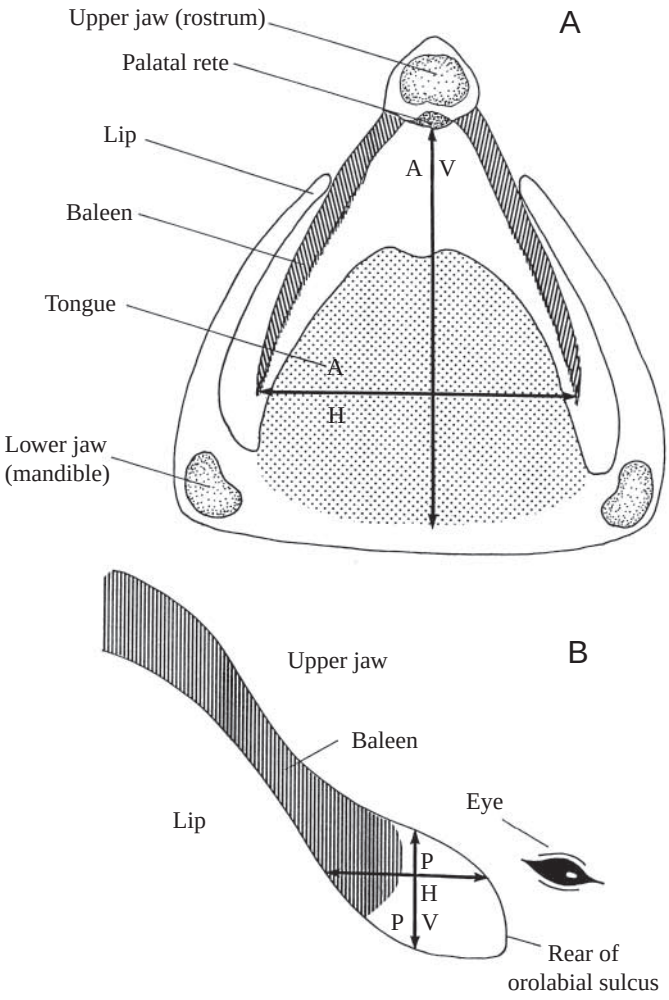

Fig. 3. Schematic diagrams showing landmarks for measurements of the bowhead mouth's anterior and posterior openings (AO and PO, respectively) used in constructing mathematical and physical models. (A) Transverse section at front of oral cavity shows the relationships of tongue, lips and baleen, and the locations of anterior vertical (dorsoventral; AV) and horizontal (frontal plane; AH) dimensions. Specific demarcations of all measures defined in text and in Table 1. (B) Lateral view at rear of mouth, showing locations of posterior vertical and horizontal (PV, PH, respectively) dimensions where filtered water exits this unidirectional flow system; compare to Fig. 1 for a wider view.

the rostrum and lip lack the high, curving arch found in adults; baleen does not grow until late in prenatal development) meant that fetal measurements could not be accurately scaled to adult size. Thus no fetal dimensions were used in constructing either the mathematical or physical model. Due to their small size, however, the fetuses still proved quite useful, as several aspects of oral anatomy that do not change shape during prenatal/postnatal growth and that demonstrate isometric growth (e.g. lingual furrow, genioglossal tubercle, orolabial sulcus) could be more closely scrutinized for consideration in assembling the 1/15 scale physical model.

Mathematical model

Rationale and design

As depicted in Fig. 1, the bowhead's capacious scoop-shaped lower jaw forms a large opening for water intake, while paired openings at the rear of the mouth (caudal to the orolabial sulci; Fig. 3) serve as exhaust ports. The resulting channels, bounded by the lips, baleen and floor of the mouth, act as oblique, elliptical conduits for water flow, analogous to a huge, irregular, Y-shaped pipe (Fig. 4). The pipe-like nature of this system lends itself to fluid dynamic analysis.

According to basic principles of hydrodynamics, the equation of continuity for fluids (an indirect statement of the law of conservation of mass) demands that the volume flow rate be the same in all parts of a pipe, so that the velocity of flow through sections with smaller cross-sectional area must increase. Bernoulli's theorem (essentially an extension of the law of conservation of energy) states that the sum of the pressure and potential and kinetic energies per unit volume must be constant at all points in streamlined flow, so that as fluid velocity increases, pressure simultaneously decreases.

Analysis

Combining several sources of information, i.e. measurements obtained during examination of freshly harvested whales, dissection of preserved fetal specimens, anatomical data concerning tongue and lip positions *in vivo*, and behavioral observations (gape, swimming speed and direction), a simple conceptual model was devised to investigate water flow in the bowhead oral cavity during continuous surface or mid-water ram filtration. This model depends on (1) the incurrent flow rate and (2) the diameter(s) of the 'pipe'. Reasonable values for both can easily be found. With this morphological and ecological information, various equations can be employed to measure the pressure differential as water flows through the bowhead oral cavity during filter feeding. All assume non-turbulent, steady state flow of incompressible fluid.

Given the information on flow velocity ($\dot{V}$) and cross-sectional areas of the anterior and posterior openings (AO and PO), the pressure differential (ΔP) between the front and back of the mouth can be calculated by a simplified version of Bernoulli's equation (Vogel, 1994):

$$\Delta P = \rho \dot{V}^2 / 2(1 - AO^2/PO^2) , \quad (1)$$

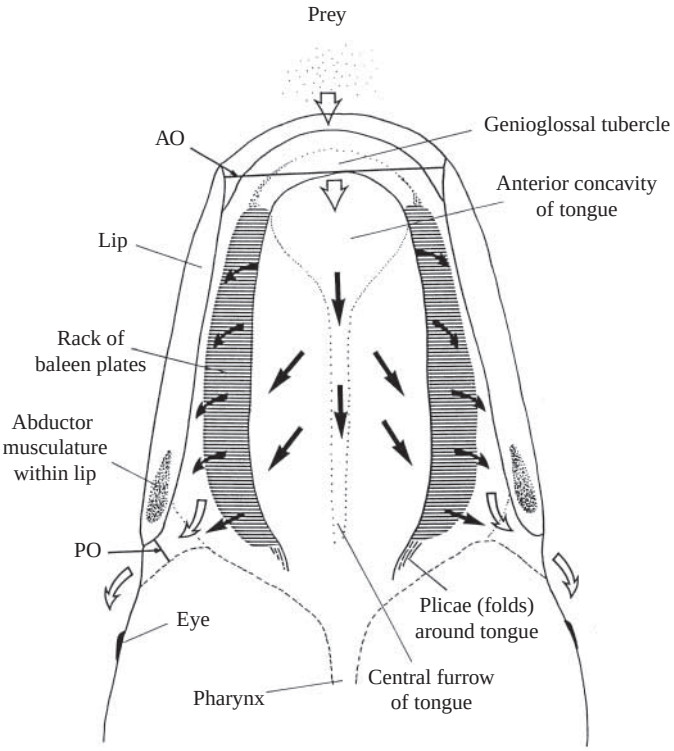

Fig. 4. Diagrammatic frontal section through the balaenid oral cavity for the model of continuous ram filtration powered by forward locomotion, showing the relationships of tongue, lips and baleen, and the flow of water-borne prey through the mouth: inward through the anterior subrostral gap between baleen racks, rearward to the center of mouth, and outward through the fringed medial side of baleen (filtration step) into the gutter-like channel inside lip (orolabial sulcus). Areas of mouth's anterior and posterior (paired) openings (AO and PO, respectively; see Fig. 2) are used in modeling. Incurrent/excurrent flow through AO and PO are shown by open arrows.

where ρ is the density of the fluid (1.024×10^3 kg m^{-3} for seawater). Bernoulli's equation holds for non-turbulent flow. While this is a reasonable assumption, considering the relatively slow flow rate and exceptional oral streamlining, boundary layers may develop in the laminar flow.

Although balaenid oral openings are manifestly non-circular, values for a pressure differential may be computed *via* formulae for flow through circular apertures at high Reynolds numbers (low viscosity, high inertia). A version of the Hagen–Poiseuille equation (Vogel, 1994):

$$\dot{Q} = C_o \pi r^2 \sqrt{(2\Delta P/\rho)} , \quad (2)$$

where C_o is a dimensionless orifice coefficient (~0.6 at high Reynolds numbers), provides volume flow rate, $\dot{Q}$. Use of this orifice coefficient (and assumption of circular anterior and posterior oral orifices) yields an admittedly simplified result, but the internal structure of the bowhead oral cavity is strikingly pipe-like. However, a more refined restatement of the Hagen–Poiseuille equation (Vogel, 1994):

$$\dot{Q} = (\pi \Delta P a^4) / (8\mu L) , \quad (3)$$

where $\dot{Q}=\Delta P/R$ and L=length, considers the resistance (R) of the flow system, taking into account the baleen's pore size and plate thickness. This resistance, as Vogel (1994) explains, characterizes laminar flow through this pipe-like system independent of pressure drop, total flow or velocity of flow.

Finally, a variation of the Navier–Stokes equation (essentially $F=m\boldsymbol{a}$, where F=force, m=mass, $\boldsymbol{a}$=acceleration), from Muller et al. (1982):

$$\Delta P = -\rho(\Delta \dot{V}/\Delta t)\Delta L \,, \quad (4)$$

relates to fluid acceleration through circular apertures, and this too can provide a rough value for the pressure drop in the oral cavity.

Physical model

Construction

A 1/15 scale model head of an adult (15 m) bowhead whale was fashioned from air-drying synthetic plastic clay stone over a lightweight armature of wire, wood and rigid polystyrene foam. Plates of 'baleen' were fabricated from pliable 18 mil high density polyethylene. The model was primed with acrylic water-based gesso prior to painting with flat spray enamel and sealing with several coats of clear polyurethane to ensure waterproofing.

The model was designed to replicate all structures of the balaenid oral cavity in proper proportions, positions and relations. The head was constructed in two sections, with an articulating upper and lower jaw, so that although the lips and tongue were immobile, the mouth could be opened and closed. The lips were created to simulate the adducted (laterally rotated) position for feeding at normal gape; the tongue was sculpted in typical elevated mid-sagittal position. Obviously, because the plastic 'baleen' was not constructed of the actual keratinous tissue (and since even this tissue would exhibit different physical properties at reduced scale), a material of suitable flexibility (HDPE: high density polyethylene) was chosen to approximate, as well as any simulated material could, the true plates' mechanical behavior and to recreate the exact dimensions of length, width and thickness with regard to scale, as well as the number of plates (300). Unfortunately the fibrous mat of interwoven medial fringes could not be precisely duplicated at this scale, yet the paramount concern was to devise a model demonstrating the specific anatomical features of the baleen sieve (e.g. convex lateral surface) that determine its filtering capability and affect intraoral water flow. Care was taken to reproduce accurately other internal features (e.g. the tongue's central furrow, anterior concavity, longitudinal plicae and genioglossal tubercle). Dimensions of the anterior and posterior oral openings were taken from the measurements obtained during the necropsy procedure from harvested whales and reduced to 1/15 scale.

Testing

The completed 35 cm model (Fig. 2) was placed (suspended on clear monofilament wire) in a 135 l flow tank (30 cm×30 cm×80 cm; working section with length of 70 cm and cross-sectional area of 900 cm^2; 11.5% blockage due to model), through which water rapidly recirculated at a rate of roughly 17 l min^{-1}. Brine shrimp *Artemia nauplii* eggs or other reflective particles and dyes were introduced to show water flow patterns as the model was videotaped in lateral, anterior and dorsal views while suspended before a ruled (1 cm^2) grid. Videotaping occurred at distances (lens to physical model) of 15–40 cm; most sequences were shot (and best spatial resolution was achieved) at a distance of 24 cm. Video sequences were shot using a Hitachi 1600A standard color VHS videocamera (30 frames per second; Hitachi Corp, Fremont, CA, USA) and analyzed frame-by-frame using a Panasonic AG-1730 ProLine Multiplex VCR (Matsushita Electric Corp., Osaka, Japan). Flow velocity was measured by video analysis of movement of the reflective particles relative to the ruled background.

Videotaped sequences were analyzed to examine flow patterns in incurrent and excurrent streams and to calculate their respective flow rates. In some trials the model was moved through the tank, in both circulating and non-circulating (stagnant) water, again on the suspension wires, at $\dot{V}$=3 cm s^{-1} (Re=1.8×10^3, with characteristic length D=30 cm and $\dot{V}$=3 cm s^{-1} in freshwater at 5°C), to duplicate the locomotion powering ram filtration. For later testing a tube was placed at the rear of the buccal cavity; suction pressures generated by a water pump or by siphoning (measured at –7.33 kPa) enabled increased water flow (230% increase, from 3 cm s^{-1} to 7 cm s^{-1}) through the oral cavity for clearer visualization of filtration and hence of the flow rate and path of reflective particles or dye.

Direct pressure measurement

Finally, intraoral pressures were directly measured in the 1/15 scale physical model to assess independently the results derived from the fluid mathematical model. Two types of pressure transducers were used. A strain-gauge based DTX Disposable Transducer (4 ms response time; Spectramed, Oxnard, CA, USA) with a bare 1 mm^2 tip oriented perpendicular to flow was situated (fixed in place and, in earlier preliminary trials, allowed to dangle) at three locations throughout the buccal cavity: at the rear of the mouth, on the tongue's median furrow; just posterior to the mouth's anterior orifice, posterior to the subrostral baleen gap; and in the orolabial sulcus lateral to the baleen but medial to the lip. Also, a 2F Millar Mikro-Tip® micromanometer-tipped catheter pressure transducer (20 ms response time; Millar Instruments, Houston, TX, USA) was used, again with a bare 1 mm^2 tip oriented vertically (dorsoventral, perpendicular to flow), and fixed in the model at the locations noted above, again with the transducer tip perpendicular to flow in the static (but close to the dynamic) component of the pressure field. Most pressures were recorded at flow velocity of 3 cm s^{-1}.

DTX transducers were calibrated and linked through ETH-400 transducer amplifiers to a MacLab A–D converter (ADInstruments, Milford, MA, USA) and recorded/analyzed at sampling rates of 100 kHz (16 bit resolution digitization)

using MacLab software on a Power Macintosh G3 computer (Apple Computers, Cupertino, CA, USA); Millar transducers were connected to the MacLab unit and calibrated *via* a TCB 500 control unit with recording at the same sampling rate.

Results

Morphometrics

Table 1 lists measurements of the five specimens used in devising the mathematical model of water flow through the bowhead oral cavity, plus measurements for the 1/15 scale physical model and the two fetal whales consulted in assembling the physical model. For these five whales, the mean L_b was 11.9 m, with a mean head length of 3.13 m. Mean (± S.E.M.) dimensions of the oral openings were: AV, 2.42±0.19 m; AH, 2.21±0.18 m; PV, 1.26±0.08 m; PH, 1.39±0.08 m. These provide, for all specimens, a mean radius of 1.16 m for the anterior opening and 0.66 m for the posterior opening (1.27 and 0.71 m, respectively, for a 'standard' 15 m whale). The minimal differences between the sagittal and frontal plane dimensions of the mouth (AV/AH) confirm the approximate circularity of this orifice.

Mathematical model

The conceptual mathematical model depends on the bowhead mouth's incurrent flow rate and the diameter of the oral 'pipe'. Regarding the former, although the speed of migrating bowheads ranges from 3–9 km h^{-1}, as measured during census tracking by theodolite or surveyor's transit (Reeves and Leatherwood, 1985), observations of feeding whales in neutral current, open water conditions (Carroll et al., 1987; Lowry, 1993; Nowacek et al., 2001) suggest a more modest foraging speed (and hence water influx velocity) of 4 km h^{-1}. This speed (4 km h^{-1}) was used for initial calculations of the mathematical model, but a faster foraging speed (6 km h^{-1}, the mean of the theodolite records of 3–9 km h^{-1}) was used in further calculations to test the effect of incurrent flow velocity.

As for the size of the oral 'pipe', published estimates of the oral opening in *Balaena* range from 1–9 m^2, yet my necropsy data conform to values presented by Thomson (1987). Based on jaw and baleen measurements and aerial photographs of skim-feeding bowheads, from which gape and lip position can be clearly seen, Thomson calculated that the anterior mouth opening (AO, in m^2) for whales of body length (L_b) 7–18 m can be ascertained by the equation:

$$AO = 9.48\times10^{-3}(L_b^{2.365}) . \quad (5)$$

For a 15 m whale this yields a value of 5.73 m^2, in line with my calculation of 5.09 m^2 for a whale (93B6, hauled out on ice) of similar length and with presumed full gape. For all adult whales used in this study the mean AO was 4.23±0.66 m^2 (± S.E.M., N=5). My calculated area for the posterior aperture of a 15 m L_b whale, again from necropsy data, is 1.57 m^2 (for all whales, mean L_b 11.9 m: PO=1.39±0.16 m^2, N=5), for a total effluent area (with two orifices, one for each lip) of 3.14 m^2

Table 1. *Morphometric data from adult and fetal bowhead whales (all specimens female) plus 1/5 scale physical model*

	Whale number					Mean ±	Fetus number		
Measurement	93B6	93B12	93B16	95B6	95B7	S.E.M. (adult)	88kk1F	90B4F	Model
L_b	14.99	10.10	11.05	9.64	13.72	11.9±2.09	1.50	3.90	Head only
L_H	3.79	2.69	2.95	2.56	3.65	3.13±0.50	0.41	1.04	0.33
L_{Ba}	2.74	1.90	1.91	1.68	2.35	2.12±0.38	0.07	0.16	0.15
L_T	4.10	2.37	3.20	2.49	3.78	3.19±0.68	0.47	1.05	0.28
W_A	0.43	0.36	0.38	0.33	0.41	0.38±0.03	0.12	0.15	0.08
H_A	1.17	1.08	1.04	1.08	1.22	1.12±0.07	0.22	0.29	0.12
H_L	2.85	1.93	2.11	1.83	2.59	2.26±0.39	0.47	0.59	0.18
AV	2.67	2.24	2.26	2.31	2.63	2.42±0.19	0.21	0.60	0.07
AH	2.42	2.05	2.17	1.99	2.40	2.21±0.18	0.19	0.64	0.075
AV/AH	1.10	1.09	1.04	1.16	1.10	1.10±1.06	1.10	0.94	0.93
PV	1.36	1.19	1.22	1.17	1.35	1.26±0.08	0.10	0.29	0.03
PH	1.47	1.35	1.37	1.29	1.49	1.39±0.08	0.12	0.35	0.04
AO	5.09	3.61	3.86	3.63	4.97	4.23±0.66	0.031	0.30	0.00413
PO	1.57	1.27	1.32	1.19	1.58	1.39±0.16	0.009	0.08	0.00096

L_b, body length = tip of rostrum to fluke notch; L_H, head length = tip of rostrum to center of blowhole; L_{Ba}, length of longest baleen plate, including gum; L_T, tongue length, tip to root; W_T, tongue width at mid-length; H_T, tongue height at mid-length; H_L, maximum lip height; AV, Anterior Vertical measurement = tip of rostrum (at subrostral gap between anteriormost baleen plates) to floor of mouth; AH, Anterior Horizontal = between tips of anteriormost baleen plates; PH, Posterior Horizontal = rear of lip to head at level of eye; PH, Posterior Vertical = bottom of orolabial sulcus to upper jaw, at approximate midline of PH; AO, calculated area of anterior opening of mouth; PO, calculated area of posterior opening of mouth, for each side.

All linear dimensions given in m; areas of anterior and posterior openings (AO and PO) are in m^2.

The unitless AV/AH value is a proxy for circularity, showing the difference between the mouth's sagittal and frontal plane dimensions.

Values are means ± S.E.M. for five adult specimens only.

in a 15 m whale. I assume these dimensions are similar for whales feeding below the surface in normal upright position (Thomson's study was based in part on aerial photographs of whales feeding at the surface on their sides). Again, this model also assumes non-turbulent, steady-state flow of incompressible fluid. In all of the calculations that follow I use AO and PO areas based solely on my measurements, as shown in Table 1. Dimensions computed from Thomson's regression equation were checked (for accuracy and precision) against my measurements but not used in any mathematical modeling.

Using the values presented above for a 15 m whale (V=4 km h^{-1}=1.11 m s^{-1}; AO=5.73 m^2; PO=3.14 m^2), Bernouilli's equation provides a pressure differential of –1026.81 Pa (–7.70 mmHg) from the front to the back of the mouth. As noted, Bernoulli's equation holds for non-turbulent flow and the calculated Reynolds number for these conditions (1.25×10^3) indicates laminar flow. At a higher foraging speed of 6 km h^{-1}, Bernouilli's equation yields a pressure differential of –2324 Pa (–17.43 mmHg) for this standard 15 m whale. Calculated values for whales of other sizes swimming at both velocities are listed in Table 2.

The simplified Hagen–Poiseuille equation 1 (using an orifice coefficient) yields a pressure of –1768 Pa for a 15 m whale at the 4 km h^{-1} foraging speed, assuming the oral opening (AO=r^2) is 5.09 m^2 (r=1.27 m) and the volume flow rate, $\dot{Q}$, is 5.65 m^3 s^{-1} (volume based on my measurements). The restatement of the Hagen–Poiseuille equation 2 using resistance (from the physical model's 'baleen' filter; R=288.14 N m^{-2}) yields a pressure differential of 1628 Pa for the same conditions. At the higher 6 km h^{-1} foraging speed, again for a standard 15 m whale, the two forms of this equation, respectively, yield –4002.7 Pa and –2449.3 Pa. Given the potential pulsatile nature of flow through the baleen mouth, the dimensionless Womersley number, α, was calculated (based on fluke stroke frequency ω=0.3, using data from Nowacek et al., 2001, 2003). This number ($\alpha=3.1\times10^3$) shows that flow is not unsteady, validating use of the Hagen–Poiseuille equation.

Finally, the Navier–Stokes equation, using a 3.8 m head length (L_H) for the oral cavity of a 15 m L_b whale with 1.11 m s^{-1} flow, yields a pressure drop of 1261.3 Pa. If foraging speed (and hence incurrent flow velocity) increases from 4 to 6 km h^{-1} for the same size whale, then this equation yields a greater negative pressure of –2856 Pa, which is more than twice the value for the slower speed. Values for whales of differing size at both speeds (Table 2) are identical to those of a 15 m whale, since head length (obtained from necropsy data) is almost perfectly proportional to L_b and since the

Table 2. *Calculations from the mathematical model using mean dimensions from all whales, as well as for whales of 5, 10, 15 and 20 m body length foraging at speeds of 4 or 6 km h^{-1}, showing pressure differential from anterior to posterior of oral cavity*

		ΔP obtained using different equations				
Length L_b (m)	Speed (km h^{-1})	Bernouilli	Hagen–Poiseuille 1	Hagen–Poiseuille 2	Navier–Stokes	Mean ± S.E.M.
Mean (11.9)	4	829.3 (6.22)	2145.3 (16.09)	1977.3 (14.83)	1261.3 (9.46)	1554.0±533.9 (11.7±4.0)
	6	1878.7 (14.09)	4857.3 (36.43)	2973.3 (22.30)	2856.0 (21.33)	3141.0±1078.1 (23.5±8.1)
0.33 m model[a]	scale 1.7	26560 (199.2)	75107 (563.3)	17970 (134.8)	13070 (98.0)	33177±24685 (248.8±185.1)
5	4	477.3 (3.58)	27418.7 (205.64)	25248.0 (189.36)	1261.3 (9.46)	13601.5±12758.0 (102.0±95.7)
	6	1080.0 (8.10)	62056.0 (465.42)	37980.0 (284.85)	2856.0 (21.33)	22411.5±24910.0 (194.9±191.3)
10	4	642.7 (4.82)	3381.3 (25.36)	3013.3 (22.60)	1261.3 (9.46)	2074.8±1150.8 (15.6±8.63)
	6	1456.0 (10.92)	7652.0 (57.39)	4684.0 (35.13)	2856.0 (21.33)	4161.8±2317.3 (31.2±17.4)
15	4	1026.8 (7.70)	1768.0 (13.26)	1628.0 (12.21)	1261.3 (9.46)	1421.0±293.5 (10.7±2.2)
	6	2324.0 (17.43)	4002.7 (30.02)	2449.3 (18.37)	2856.0 (21.33)	2908.0±662.1 (21.8±4.9)
20	4	641.3 (4.81)	1385.3 (10.39)	1274.7 (9.56)	1261.3 (9.46)	1140.8±292.5 (8.6±2.2)
	6	1450.7 (10.88)	3134.7 (23.51)	1917.3 (14.38)	2856.0 (21.33)	2339.5±683.0 (17.5±5.1)
Mean ± S.E.M.[b]		1180.5±563.5 (8.86±4.2)	11780.1±18286.9 (88.35±137.15)	8214.0±11781.1 (62.36±90.2)	2059.0±797 (15.39±5.9)	[5475.4±6622.9 (43.8±56.7)]

[a]Head length L_H, not total body length L_b, which would be ~1 m of 1/15 model.

[b]Only for actual whales; does not include 1/15 scale physical model.

ΔP, pressure differential (Pa; values in mmHg are given in parentheses).

Hagen–Poiseuille equations 1 and 2, see text for explanation.

Also shown are calculations, from the mathematical model, for the 1/15 scale physical model at the speed of its flow tank testing.

All values are for negative pressures (less than ambient).

Navier–Stokes equation deals with fluid acceleration and thus flow velocity.

While the latter pressure values (from the Hagen–Poiseuille and Navier–Stokes equations) are derived from equations relating to fluid acceleration through circular apertures, they corroborate the Bernoulli calculation of –1467 Pa and confirm that it is in the proper order of magnitude. All iterations of the mathematical model yield a pressure differential, from the front to the rear of the filtering bowhead's oral cavity, on the order of –1300 Pa for the default scenario of a 15 m whale foraging at 4 km h^{-1}. Pressure differentials increase as foraging speed increases, and are generally higher in larger whales, though this depends on the formula(e) used. [As I did not have a 5 m long necropsy specimen to measure, values for that L_b in Table 2 are rough approximated extrapolations based on the 15 m 'standard' adult and the near-term 3.9 m fetus, although it is acknowledged that, as mentioned, the latter displays allometric scaling.] All conditions tested in the mathematical modeling reflect laminar flow, fulfilling the assumptions of the formulae.

Physical model

Visualization of flow and filtration

Water flow upstream of the model (again, measured by video analysis of particle or dye movement) occurred at a velocity of 2.72±0.23 cm s^{-1} (mean ± S.E.M., N=31). Water and particles could be seen entering the mouth at a mean flow velocity of 3.18±0.39 cm s^{-1} (N=16) and exiting through the smaller posterior opening(s) at a mean flow velocity of 4.84±0.47 cm s^{-1} (N=16); Fig. 5B. These rates are derived from flow through a stationary model. However, forward movement of the physical model (at 3 cm s^{-1}) through neutral current conditions yielded similar flow velocities. When scaled to full size this locomotor velocity, 3 cm s^{-1} for the 1/15 scale model, translates to only 48 cm s^{-1} (1.73 km h^{-1}), less than half the 4 km h^{-1} swimming speed (1.11 m s^{-1}) used in the mathematical model, yet the tank was too small to allow forward motion at 1/15 scale (7.5 cm s^{-1}) for more than 7 or 8 s. Because intermittent movement of the model for short durations could affect flow dynamics by introducing acceleration effects, I present here only data from a stationary model. Still, in no sequences were particles 'pushed' ahead or to the sides of the model by a compressive bow wave, even with a moving model.

Water clearly flowed from the posterior mouth openings more rapidly than it entered the larger anterior opening. Water/particle flow is best seen in dorsal view, where it is apparent that some particles pass through the mouth but many are trapped in the 'baleen', whose fringes, as noted, could not be made as extensive as in life. [Because the balaenid rostrum is so narrow, and because baleen angles outward (medially) from the rostrum, baleen can easily be seen in dorsal view.] Though the lips were immobile, gape could be altered. When the upper jaw was raised too high, i.e. at a gape angle of greater than about 25°, the rostrum created turbulence and fewer particles were captured in the 'baleen'.

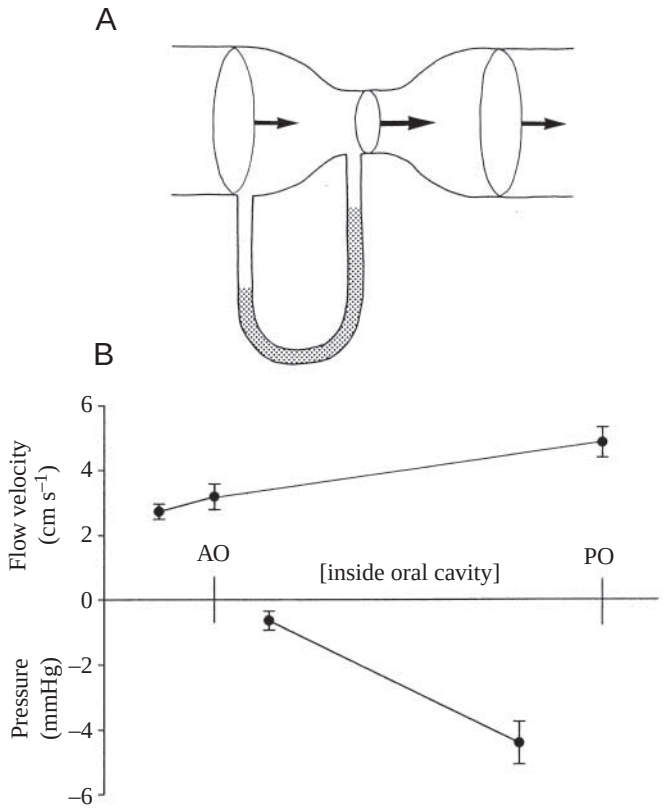

Fig. 5. Elementary fluid dynamics serves as the basis for mathematical and physical modeling. If volume flow rate holds constant as the diameter (and hence cross-sectional area) of the flow pipe decreases, flow velocity increases and pressure decreases. (A) Venturi manometer showing pressure drop as flow speed increases through the constriction in the pipe. (B) Flow tank data from 1/15 scale physical model showing changes in flow rate (recorded *via* videotape) as water moves from the upstream current through the anterior opening (AO) and out *via* the posterior opening (PO), plus pressures (recorded *via* transducers) at front and back of the oral cavity, showing a drop of 501 Pa (3.76 mmHg). Values are means ± S.E.M.

Mathematical modeling was also performed using the parameters of the physical model's flow tank testing. Resulting values are displayed in Table 2.

Direct pressure measurement

Both types of transducer yielded similar values for direct measurement of pressures, though only fixed attachment (not dangling transducers) generated conclusive results. Although pressures could be recorded at the anterior and posterior oral locations (on the rostrum just posterior to the subrostral baleen gap, and at the rear of the mouth above the root of the tongue, respectively, with transducer tip perpendicular to flow), measurement from the orolabial sulcus did not yield significant pressure changes, positive or negative. Pressures recorded from the front of the mouth were only slightly less than ambient (–87±0.29 Pa; mean ± S.E.M., N=38), but those from the rear location were significantly lower (–588±0.66 Pa; mean ± S.E.M., N=38; both recorded at flow velocity=3 cm s^{-1}). Thus

there was a mean pressure differential, from the anterior to the posterior of the mouth, of 500 Pa or –3.76 mmHg (Fig. 5B). Although this value is lower than those derived from the mathematical model (–1469 Pa from Bernouilli's equation; –1499 Pa and –1628 Pa from the Hagen–Poiseuille equations, –1262 Pa from the Navier–Stokes equation), it is in the same order of magnitude, and, as with the qualitative observations of the physical model, serves to corroborate the results of the mathematical model.

In the few trials in which the physical model's gape was altered (generating turbulent flow, as described above) recorded pressures dropped markedly. Direct pressure measurement varied slightly yet not significantly (P=0.36) with flow velocity. As the upstream flow velocity increased from 3 cm s^{-1} to 5 cm s^{-1}, the pressure differential (front to rear of mouth) increased from –461±57 Pa (mean ± S.E.M., N=12) to –543±109 Pa (mean ± S.E.M., N=12), again supporting the fluid mathematical model. Volume flow rate of the test tank could not be altered sufficiently for conclusive experimentation.

Discussion

Both mathematical and physical modeling support the contention that hydrodynamic pressure effects influence flow and filtration processes in the bowhead mouth. Measurement of particle flow from the scale model demonstrates clear continuity effects. The morphology of the balaenid oral cavity accelerates water flow in ways that may avoid formation of a compressive bow wave and hence prevent escape of small prey. It may also facilitate prey transfer from water to baleen, as by inertial deposition of suspended items (Rubenstein and Koehl, 1977). Both the mathematical and physical models rely on the narrowing channel above the orolabial sulcus coupled with water flow into the middle of the mouth (between medial baleen surfaces) to replace low pressure water flowing out caudal to the lip. As this channel narrows and its cross-sectional area decreases, flow speed increases and pressure decreases (Bernoulli effect). As pressure at the orolabial sulcus decreases, water rushes to the orolabial sulcus (outward, from the center of the mouth) perpendicular to this longitudinal flow (laterally, between baleen plates) to fill this space (the Venturi effect; Fig. 5A). The result is pressure-induced flow through the sieving apparatus, so that filtration is powered by hydrodynamic as well as hydraulic pressures, as Lambertsen et al. (1989) postulated. Just as a nozzle at the end of a garden hose increases the velocity of water flow, the constriction at the rear of the bowhead buccal cavity increases fluid flow rate while holding the flow volume constant (Fig. 5B). The ratio of entrance to exit flow velocities measured in testing of the physical model conforms to expectations based on continuity.

The mathematical model suggests an intraoral pressure drop of roughly 1420 Pa (11 mmHg) in a 15 m whale swimming at 4 km h^{-1} and approximately twice that (2910 Pa) in a 15 m whale swimming at 6 km h^{-1}. Results from the physical model (Fig. 5B) are complementary to those of the mathematical model (Fig. 6), both quantitatively (a drop of ~500 Pa, from direct pressure measurement in a stationary model and in a moving one at speed scaling to 1.7 km h^{-1}) and qualitatively (higher exit flow velocity; 'pulling' of particle-laden water in anteriorly with no compressive bow wave; maintenance of laminar flow). All flow involves pressure changes, but the correspondence of pressure measurements from the fluid and scale models suggest that the flow of water through the bowhead whale filtration system is pipe-like.

Sensitivity analysis is important in any simulation study. Clearly the two principal variables of this continuous ram filtration system (morphometric dimensions and foraging speed) are sensitive to variance. Results from the fluid mathematical modeling indicate that in all cases as foraging

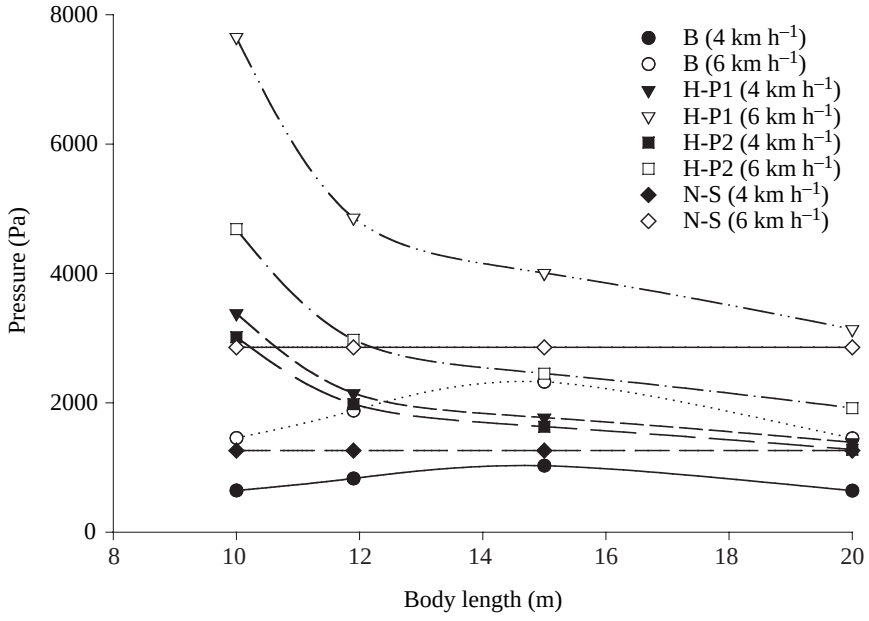

Fig. 6. Data (from Table 2) showing results of fluid mathematical modeling for whales of varying body length foraging at speeds of 4 km h^{-1} (solid symbols) or 6 km h^{-1} (open symbols). Pressure differential values were derived from four equations: Bernoulli (circle), two formulations of Hagen–Poiseuille (triangle, square) and Navier–Stokes (diamond). Calculations for L_b=5 m are not included here, as these were based on extrapolated morphometric data. For comparison, there was a mean 500 Pa pressure drop, measured *via* transducer, in the flow tank testing of the 1/15 scale physical model (33 cm head length; equivalent of L_b ~1 m).

velocity (and hence incurrent flow velocity) increases, the pressure differential is greater (Fig. 6). Also, body size plays a factor. With both formulations of the Hagen–Poiseuille equation, the intraoral pressure drop was substantially greater the smaller the whale. Because most of the measurements were taken from whales with L_b = 10–15 m, and since the 1/15 scale physical model was based on dimensions of a 15 m whale, results for this size are likely to be more accurate. Data for smaller whales are particularly suspect (especially for both iterations of the Hagen–Poiseuille formula) since, as explained earlier, a very young 5 m whale was not available for necropsy; calculations for L_b = 5 m (and 20 m) are rough extrapolations from other whales (these data are provided in Table 2 merely for comparison). For whales in the 10–15 m size range, however, all of the various formulae of the mathematical model yield consistently similar results, again suggesting decreased intraoral pressures on the order of (at least) 1300–2700 Pa (10–20 mmHg). It is important to note once again that the foraging gape and speed values were taken from observation and measurement of feeding whales, just as the necropsy measurements came from real whales.

Both models validate the predicted hydrodynamic flow in relative terms, but the values may not reflect estimates of flow velocity and pressure that can be scaled directly to a living whale. The range of variation in pressure values that might reasonably be generated by realistic variation in morphometrics and swimming velocity in a 10–15 m whale likely ranges from –1.3 kPa to –13.3 kPa. This is admittedly not a huge drop in pressure, though it ought to be sufficient to improve filtration (if not greatly) and augment the simple hydraulic effects (balaenid whales do not engulf prey *via* suction, as does the gray whale, *Eschrichtius robustus*). It must be emphasized, however, that both aspects of this model of the bowhead filtration system conclusively demonstrate reduced intraoral pressures *via* the Bernouilli and Venturi effects; it seems clear that the decrease in pressure is real and significant.

Running the fluid mathematical model using conditions of the physical model served to ‘ground-truth’ the modeling. Although this yielded pressure differentials higher than those calculated with ‘real’ whale measurements (Table 2), this is not surprising since body length is a critical factor, and the model represented a total L_b of just 1 m. Some near-term bowhead fetuses are five times this length (Koski et al., 1993). Plugging the physical model into the mathematical model yielded results (for most equations) in the same order of magnitude as of the smallest whales shown in Table 2. The mean intraoral pressure drop, for all equations, for the physical model ‘swimming’ in the flow tank condition of a scale equal to 1.7 km h^{-1} was –33.2 kPa; for that of a 5 m whale at 4 km h^{-1}, –13.6 kPa or about half as much. Further, when a purely hypothetical 1 m whale (again, much smaller than the average newborn bowhead of 4.3 m; Koski et al., 1993) is used for the mathematical modeling, the results are similar to those using values for the 1 m scale model. Relating the two models helps to put conclusions about large scale, real world pressure changes on firmer footing. It not only validates the pressure calculations and assumptions but also provides further qualitative and quantitative information about continuity effects. However, one must be very careful when assuming that pressures measured (and calculated) from the 1/15 scale model would be identical to those of a real whale swimming at higher speed under different Reynolds conditions. This modeling is limited by the simplicity of its assumptions, particularly when considering if the models have true predictive value in absolute terms.

Due to the slick, streamlined nature of the pipe-like oral channel and the steady, relatively slow speed of flow, it is unlikely that turbulence is generated; the models’ laminar, frictionless conditions are validated. It is important to consider differences in fluid force scaling from real filtering whales to the physical model head in the flow tank (with smaller size and lower velocities), yielding a one thousand-fold difference in Reynolds number (1.8×10^3 for the model; 2.5×10^6 for actual whales at the feeding velocity used in this study; flow velocity in the test tank could not be scaled perfectly to the latter *Re*). The lower *Re* value reflects laminar pipe flow. The larger figure, for real whales, reveals flow that could be transitioning to turbulent, and this would have major implications for the equations of the mathematical model that assume laminar flow. Of course, the *Re* regime would differ in feeding whales depending on swimming speed and gape (and hence dimensions of the oral pipe), though neither factor is expected to vary appreciably. Changes in the baleen filter (particularly fringe density and thus porosity and resistance, *R*) would also affect flow velocity and thus alter *Re*. Even though the *Re* values vary by three orders of magnitude, both are in the realm of inertial dominance, substantiating the presumption of Bernoulli flow parameters.

The pipe-like nature of the bowhead’s continuous filtration system presents an opportunity to calculate the mechanical cost of its filter feeding based on pressure–volume work. Most of the work measured in the pressure drop is likely due to the resistance of the baleen filter. Using the pressure differential from the Bernoulli equation calculations, one can back out the resistance in the Hagen–Poiseuille equation and, after removing pipe length and diameter effects, estimate the resistance added by the baleen. This yields estimates of resistance of R=146.7 N m^{-2} for a whale foraging at 4 km h^{-1} and R=332.6 N m^{-2} for a whale foraging at 6 km h^{-1}. These values compare quite favorably to the resistance measured from the 1/15 scale physical model’s ‘baleen’ filter, cited earlier, of R=288.14 N m^{-2}. Again there is concordance between the two models.

In their study of bowhead baleen contours, Lambertsen et al. (1989) proposed that the curved cross-sectional shape of each plate as well the laterally bowed profile of each baleen rack might accentuate a pressure gradient, resulting in improved filtering efficiency. The characteristic sluggishness of balaenids is often ascribed to the giant filter’s high resistance to water flow, generating pressure drag that severely slows

feeding whales and prohibits capture of large or evasive prey (Sanderson and Wassersug, 1990). Reduced intraoral pressure could negate the compressive effect of the forward locomotion powering this system, perhaps allowing balaenids to swim faster and alleviating or entirely eliminating bow waves that disperse prey or prompt prey to take evasive action. However, frictional drag would increase as a square of velocity, adding to the forward resistance and thus likely keeping swimming speed low. Würsig and Clark (1993) suggested that bowheads also benefit from foraging in tight V-shaped echelons that apparently limit prey escape. The Bernoulli and Venturi effects may produce anterior suction (albeit of negligible pressure) for prey capture; the ~1500–3000 Pa values furnished by the mathematical model for a 15 m whale would certainly prove sufficient to draw in typical (minute) prey items or at least prevent their escape. Again, continuity effects might also aid in capture of particles flowing through the oral cavity (Rubenstein and Koehl, 1977).

As Vogel (1994) noted, a swimming fish with open mouth resembles a Pitot tube. Velocity changes outside the head (*via* the Bernouilli effect) create a pressure gradient, with water entering at the mouth at the point of high pressure and exiting (posterior to the gills) at lower pressure. This serves to enhance and facilitate both ram ventilation and ram feeding. Given that balaenid (bowhead and right) whales, unlike other mysticetes, have continuous ram filtration with the buccal cavity open at the front and back, as in fishes, the same phenomenon should apply. Velocity changes outside the head should create a complementary mechanism to the one in operation internally to augment filtration further.

Clearly, the balaenid filter feeding mechanism is not as straightforward as is commonly described. Since baleen is not a rigid material, filter porosity varies according to such hydrodynamic factors as swimming speed, size and density of prey, and direction and pressure of water flow (Sanderson and Wassersug, 1990). Other elements of this continuous filtration system demonstrate complex mobility. The muscular balaenid tongue is often implicated in removal of captured prey from baleen, yet underwater footage of right whales *Eubalaena glacialis* shows the elevated tongue sweeping laterally, perhaps to direct water flow into the baleen (Werth, 1990, 2000). It is possible that hydrodynamic effects could be preferentially increased on either side of the oral cavity. Unfortunately, exceptionally low visibility at high prey densities precludes filming of this behavior. The large, mobile lip and mandible (with unfused symphysis) also play critical roles in feeding. Fibers of the temporalis muscle insert in the lip (Fig. 4) to allow outward rotation, establishing the gutter-like channel lateral to the baleen.

Due to the many legal and logistical limitations, studies of large marine mammals require ingenuity and resourcefulness. In the absence of direct experimental evidence, and with only limited, anecdotal observational evidence, modeling provides a convenient tool to investigate cetacean functional morphology. Future use of a larger flow tank and a transparent physical model would allow for more direct observation of interior flow fields. Likewise testing of this model at different locations in the water column, including surface and half-submerged positions (as is common, though far from exclusive, in bowhead feeding) should indicate the influence of gravity, if any, on these hydrodynamic effects.

List of symbols and abbreviations

$\boldsymbol{a}$	acceleration
AH	anterior frontal or horizontal
AO	cross-sectional area of the anterior opening
AV	anterior dorsoventral or vertical
C_o	dimensionless orifice coefficient
D	characteristic length (of pipe)
F	force
HDPE	high density polyethylene
H_L	maximum lip height
H_T	tongue height at mid-length
L	length
L_b	body length
L_{Ba}	length of longest baleen plate
L_H	head length
L_T	tongue length
m	mass
P	pressure
PH	posterior horizontal
PO	cross-sectional area posterior opening
PV	posterior vertical
$\dot{Q}$	volume flow rate
R	resistance
Re	Reynolds number
$\dot{V}$	flow velocity
W_T	tongue width at mid-length
α	Womersley number
ω	fluke stroke frequency

Two anonymous reviewers supplied much constructive criticism that greatly improved the content and organization of this paper, especially in terms of morphometrics and analysis of the fluid mathematical modeling. Their suggestions significantly enhanced the paper's clarity and scope. R. H. Lambertsen provided valuable information, suggestions and criticism on bowhead morphology, feeding and hydrodynamics, as did T. F. Albert, J. C. George, D. J. Hillmann and T. J. Ford. R. H. Lambertsen and M. E. Peterson also provided the reference to Fabricius and its translation from Latin. I am also grateful to D. D. Lewis for artistic advice, S. A. Cheyne for discussions of physics, and C. M. Newman and B. L. White for assistance in testing and photographing the physical model. Portions of this research were funded by a grant from the North Slope Borough Department of Wildlife Management of Barrow, Alaska (Contract No. C2189). The NSB/DWM and Alaska Eskimo Whaling Commission generously supplied logistical support and access to harvested whales. D. J. Hillmann provided access to and assistance with fetal specimens at LSU.

References

Albert, T. F. (1981). Project management, coordination of research efforts, and collection of tissue specimens from the bowhead whale, *Balaena mysticetus*, and the gray whale, *Eschrichtius robustus*. In *Tissue Structural Studies and Other Investigations on the Biology of Endangered Whales in the Beaufort Sea* (ed. T. F. Albert), pp. 19-42. Report by the Department of Veterinary Science of the University of Maryland to the Bureau of Land Management, US Department of the Interior, Anchorage, AK, USA.

Becker, P. R., Wise, S. A., Koster, B. J. and Zeisler, R. (1991). Alaska marine mammal tissue archival project: Revised collection protocol. Report **4529** of the National Institute of Standards and Technology (NISTIR), US Department of Commerce, Gaithersburg, MD, USA.

Carroll, G. M., George, J. C., Lowry, L. F. and Coyle, K. O. (1987). Bowhead whale (*Balaena mysticetus*) feeding near Point Barrow, Alaska, during the 1985 spring migration. *Arctic* **40**, 105-110.

Fabricius, O. (1780). *Fauna Groenlandica*. Copenhagen: Johann Gottlob Rothe.

Koski, W. R., Davis, R. A., Miller, G. W. and Withrow, D. E. (1993). Reproduction. In *The Bowhead Whale* (ed. J. J. Burns, J. J. Montague and C. J. Cowles), pp. 239-274. Lawrence, KS: Society for Marine Mammalogy.

Lambertsen, R. H., Hintz, R. J., Lancaster, W. C., Hirons, A., Kreiton, K. J. and Moor, C. (1989). Characterization of the functional morphology of the mouth of the bowhead whale, *Balaena mysticetus*, with special emphasis on the feeding and filtration mechanisms. Report to the Department of Wildlife Management, North Slope Borough, Barrow, AK, USA.

Lowry, L. F. (1993). Foods and feeding ecology. In *The Bowhead Whale* (ed. J. J. Burns, J. J. Montague, and C. J. Cowles), pp. 201-238. Lawrence, KS: Society for Marine Mammalogy.

Muller, M., Osse, J. W. M., and Verhagen, J. H. G. (1982). A quantitative hydrodynamical model of suction feeding in fish. *J. Theor. Biol.* **95**, 49-79.

Nowacek, D. P., Johnson, M. P., Tyack, P. L., Shorter, K. A. McLellan, W. A. and Pabst, D. A. (2001). Buoyant balaenids: the ups and downs of buoyancy in right whales. *Proc. R. Soc. Lond. B* **268**, 1811-1816.

Nowacek, D. P., Johnson, M. P. and Tyack, P. L. (2003). North Atlantic right whales (*Eubalaena glacialis*) ignore ships but respond to alerting stimuli. *Proc. R. Soc. Lond. B* **271**, 227-231.

Pivorunas, A. (1979). The feeding mechanism of baleen whales. *Am. Sci.* **67**, 432-440.

Reeves, R. R., and Leatherwood, S. (1985). Bowhead whale, *Balaena mysticetus* Linnaeus, 1758. In *Handbook of Marine Mammals*, vol. 3: *The Sirenians and Baleen Whales* (ed. S. H. Ridgway and R. J. Harrison), pp. 305-344. San Diego: Academic Press.

Rubenstein, D. I., and Koehl, M. A. R. (1977). The mechanisms of filter feeding: Some theoretical considerations. *Am. Nat.* **111**, 981-994.

Sanderson, S. L. and Wassersug, R. (1990). Suspension-feeding vertebrates. *Sci. Am.* **262**, 96-101.

Thomson, D. H. (1987). Energetics of bowheads. In *Importance of the Eastern Alaska Beaufort Sea to Feeding Bowhead Whales, 1985-86*, pp. 417-448. Report by LGL Ecological Research Associates to the OCS/Minerals Management Service, US Department of the Interior, Anchorage, AK, USA.

Vogel, S. (1994). *Life in Moving Fluids: The Physical Biology of Flow*, 2nd edn. Princeton, NJ: Princeton University Press.

Werth, A. J. (1990). Functional anatomy of the right whale tongue [Abstract]. *Am. Zool.* **30**, 21A.

Werth, A. J. (2000). Marine Mammals. In *Feeding: Form, Function and Evolution in Tetrapod Vertebrates* (ed. K. Schwenk), pp. 475-514. New York: Academic Press.

Werth, A. J. (2001). How do mysticetes remove prey trapped in baleen? *Bull. Mus. Comp. Zool.* **156**, 189-203.

Würsig, B., and Clark, C. (1993). Behavior. In *The Bowhead Whale* (ed. J. J. Burns, J. J. Montague and C. J. Cowles), pp. 157-199. Lawrence, KS: Society for Marine Mammalogy.